



# PDL and CD insensitive low complexity equalizer for short reach coherent systems

ZHENMING YU,<sup>1</sup> YILUN ZHAO,<sup>1</sup> SHAOHUA HU,<sup>2</sup> ZHIQUAN WAN,<sup>1</sup>  
LIANG SHU,<sup>1</sup> JING ZHANG,<sup>2</sup> AND KUN XU<sup>1,\*</sup>

<sup>1</sup>*State Key Laboratory of Information Photonics and Optical Communications, Beijing University of Posts and Telecommunications, Beijing, 100876, China*

<sup>2</sup>*Key Laboratory of Optical Fiber Sensing and Communications, University of Electronic Science and Technology of China, Chengdu, 611731, China*

\*[xukun@bupt.edu.cn](mailto:xukun@bupt.edu.cn)

**Abstract:** We propose a polarization dependent loss (PDL) and chromatic dispersion (CD) insensitive, low-complexity adaptive equalizer (AEQ) for short-reach coherent optical transmission systems. The AEQ contains a 1-tap butterfly finite impulse response (FIR) filter and two N-tap FIR filters. It first performs polarization demultiplexing using the 1-tap filter, of which the coefficients are obtained based on Stokes space. Then it mitigates the inter-symbol interference (ISI) using the two N-tap finite impulse response (FIR) filters and adjust the filter's coefficients by utilizing constant modulus algorithm (CMA). Through theoretical and experimental analysis, we verify that this proposed AEQ can perform robust polarization demultiplexing when PDL and CD exists. Besides, our proposed AEQ has faster convergence speed compared with recently proposed AEQs. In addition, it reduces the number of multipliers and thus reduce the computational complexity of conventional butterfly filter structure AEQ. And this proposed AEQ suffers little bit error ratio loss compared with the conventional AEQ. Due to the low-complexity and robustness to PDL and CD, this proposed AEQ is well-suited for future low-cost short-reach optical communication system.

© 2021 Optical Society of America under the terms of the [OSA Open Access Publishing Agreement](#)

## 1. Introduction

Digital signal processing (DSP) plays an important role in the newly developed digital coherent receiver, it provides us with new capabilities that were not possible without the detection of the phase of the optical signal [1]. While coherent DSP is widely used in regional or longer links, intensity modulation and direct detection (IMDD) technique is always the priority in short-reach optical communication systems such as intra/inter-datacenter and access network [2,3]. However, the limited bandwidth hinders the further increase of throughput of IMDD system. Recent studies have indicated the potentials and feasibilities of coherent techniques for future high-speed intra-datacenter optical interconnects [4–6]. Although advanced algorithms of DSP can compensate for various linear and nonlinear impairments, the complexity and thus power consumption are a major challenge for short-reach applications. Therefore, it is critical to further reduce DSP complexity.

For long-haul optical communications, the major circuit complexity comes from the compensation of fixed chromatic dispersion (CD) and the decoding of forward error correction (FEC). In the case of short-reach systems, since the smaller cumulative CD can be compensated by adaptive equalization (AEQ) and the decoding complexity of FEC can be eliminated by using hard-decision FEC, the main complexity of DSP comes from the AEQ [7]. Therefore, it is important to reduce the complexity of AEQ to achieve a more efficient DSP for short-reach systems. AEQ plays a vital role in coherent DSP flow since it is designed for both linear equalization and polarization demultiplexing (PolDemux). A typical AEQ consists of four complex-valued finite impulse response (FIR) filters with a butterfly configuration (hereinafter called conventional-AEQ). In

order to reduce its complexity, K. Matsuda *et al.* proposed a simple AEQ (hereinafter called 1tap-AEQ) configuration with a 1-tap butterfly equalizer, which is sensitive to the timing skew between in-phase (I) and quadrature (Q) or X-polarized and Y-polarized tributary channels [7]. In addition, J. Cheng *et al.* further simplified 1tap-AEQ by replacing the N-tap complex-valued filters with the real-valued filters and introduced a 3-tap T-spaced  $4 \times 4$  MIMO real-valued FIR filters for the skew compensation [8,9].

These methods perform PolDemux based on the constant modulus algorithm (CMA). However, when the polarization dependent loss (PDL) in a system cannot be ignored, CMA suffers from failure of PolDemux due to singularity problem [10]. PDL induces random SNR unbalance between the polarization tributary and such unbalance cannot be fully equalized by AEQ [11] and has been regarded as a major distortion in dual-polarization system [12,13]. As the short reach optical communication system is evolving from IMDD systems to coherent systems, it is significant for us to consider the PDL of such systems when designing AEQs. PDL can be introduced by polarization beam combiner (PBC), polarization beam splitter (PBS), wavelength selective switch (WSS) and other non-ideal polarization dependent optical devices during transmission, which could not be neglected even in the short reach networks. Besides, the authors in [9] reported that their proposed AEQ can transmit at most 8 km with less than 1 dB penalty, which limited the extensivity of AEQ to systems with longer transmission distance such as access network [7]. They explained that this penalty came from the IQ crosstalk caused by CD. However, in our research, we will further verify that this penalty also comes from the difficulty of PolDemux by 1-tap CMA. On the other hand, the PolDemux technique based on Stokes space has been well studied [14–16] and is not affected by PDL and CD, this method can perform stable PolDemux. Hence, we are motivated to take the advantage of both Stokes space and CMA. To our best knowledge, we propose for the first time a novel AEQ based on Stokes space (hereinafter called SS-AEQ), which can perform robust PolDemux and mitigate inter-symbol interference (ISI) simultaneously. Through simulation and experiment, our work makes the following contributions. (i) We propose for the first time a novel SS-AEQ and verify its performance both in simulation and experiment. Compared with 1tap-AEQ and conventional AEQ, it has a better tradeoff between PolDemux performance, convergence speed, computational complexity and bit error ratio (BER) performance. Thus we provide an alternative AEQ scenario for short reach coherent systems. (ii) In experiment and additional numerical analysis, we provide a comprehensive performance comparison between SS-AEQ, conventional-AEQ and 1tap-AEQ. We analyze the BER performance of different AEQs in a system with different PDL values, transmission distances and optical signal-to-noise ratios (OSNRs). Thus we provide readers with the basis for the selection of AEQ in short reach systems.

The organization of this paper is as follows: section 2 describes the operating principle of proposed method. We first review the theory of PolDemux in Stokes space, and the theory of conventional CMA-based AEQ. Then we review the recent progress in simplified 1-tap AEQs and discuss how this progress inspired our research. Next we introduce the principle of SS-AEQ. Section 3 verifies the performance of SS-AEQ and compare it with 1tap-AEQ and conventional-AEQ. Section 4 analyzes the tolerance of PDL and CD for different AEQs and section 5 concludes the paper.

## 2. Operating principle

The polarization rotation of the transmission in a fiber can be represented by a unitary matrix  $\mathbf{M}$ , which is independent of optical frequency:

$$\mathbf{M} = \begin{pmatrix} a & b \\ -b^* & a^* \end{pmatrix}. \quad (1)$$

Where  $a$  and  $b$  are complex and the determinant of  $\mathbf{M}$  is equal to 1. In [14], the authors proposed a method to find the inverse matrix by mapping the signal to Stokes space. We denote the received Jones vector by  $1/\sqrt{2}(e_x, e_y)^T$  and then it is transformed to Stokes vector:

$$S = \begin{pmatrix} s_0 \\ s_1 \\ s_2 \\ s_3 \end{pmatrix} = \frac{1}{2} \begin{pmatrix} e_x e_x^* + e_y e_y^* \\ e_x e_x^* - e_y e_y^* \\ e_x^* e_y + e_x e_y^* \\ -j e_x^* e_y + j e_x e_y^* \end{pmatrix}. \quad (2)$$

Where  $s_0$  represents the total power,  $(s_1, s_2, s_3)^T$  represent  $0^\circ$  linear,  $45^\circ$  linear and circularly polarized light. Next we apply singular value decomposition (SVD) theory to find the least squares plane (LSP) of Stokes vectors in Poincare sphere [16]. The normal of LSP is  $P : (p_1, p_2, p_3)^T$  and then the inversed matrix  $\mathbf{M}^{-1}$  is expressed as

$$\mathbf{M}^{-1} = \begin{pmatrix} \cos\left(\frac{\alpha}{2}\right) \exp\left(j\frac{\Delta\phi}{2}\right) & \sin\left(\frac{\alpha}{2}\right) \exp\left(-j\frac{\Delta\phi}{2}\right) \\ -\sin\left(\frac{\alpha}{2}\right) \exp\left(j\frac{\Delta\phi}{2}\right) & \cos\left(\frac{\alpha}{2}\right) \exp\left(-j\frac{\Delta\phi}{2}\right) \end{pmatrix}. \quad (3)$$

Where  $\Delta\phi = \arctan(p_3, p_2)$ , and  $\alpha = \arctan(p_2^2 + p_3^2, p_1)$ . Then the inversed matrix is utilized to perform PolDemux. Similar to the method above, PolDemux can also be achieved by a two-by-two matrix controlled by CMA algorithm. Rather than computing the inversed matrix directly, the underlying principle of this method is to iteratively update the matrix elements by minimizing the difference between the intensity of received optical waves and reference power, i.e. the constant modulus. Here we denote the two-by-two matrix by  $\mathbf{H}$ , and the matrix elements is updated iteratively by a well-known complex gradient descent formula:

$$\mathbf{H}_{i+1} = \mathbf{H}_i - \mu \varepsilon_i \mathbf{X}^H. \quad (4)$$

Where  $i$  denotes the iteration number,  $\mu$  is the step size,  $\varepsilon_i$  is the deviation from constant modulus and  $\mathbf{X}$  is the vector that contains received sample values. This method can be easily extended to multi-modulus algorithm (MMA) and is adapted to different modulation formats. Moreover, the two-by-two matrix can be extended to a  $N$ -tap butterfly filter as shown in Fig. 1, which is able to perform PolDemux and inter-symbol interference (ISI) mitigation simultaneously. Therefore, the CMA-based AEQ (i.e. the conventional-AEQ) has become a commonly used method in current DSP flow of coherent optical communication system.

Based on the two conventional methods above, we are inspired to consider combining them together and maximizing both of their advantages. Recently, multiple literatures considered the application of conventional-AEQ in short-reach coherent system and aimed at reducing its complexity to address the problem of cost. They have proposed several simplified AEQ structures that are more hardware efficient [7,8]. The key insight of their solutions is to adopt a 1-tap filter at the front of whole AEQ structure (as shown in Fig. 1(a)). It has been verified that in short-reach coherent system, a 1-tap butterfly filter is enough to perform PolDemux. Retaining the ability to perform PolDemux, this 1-tap configuration also significantly reduces the computational complexity. However, both of their solutions suffer from performance reduction and are more PDL and CD sensitive to some extent (which will be verified in section IV). We notice that this 1-tap filter regresses to a 2-by-2 matrix and the value of its elements can also be determined by Stokes-based method as we mentioned before. Hence, we propose a novel structure of AEQ, which we refer to as SS-AEQ. As depicted in Fig. 1(b), the structure of SS-AEQ is actually the same as 1tap-AEQ. However, rather than utilizing CMA to adjust the value of filter coefficients, we take the advantage of PolDemux in Stokes space, and the filter coefficients are replaced by the elements of inversed matrix  $\mathbf{M}^{-1}$ .

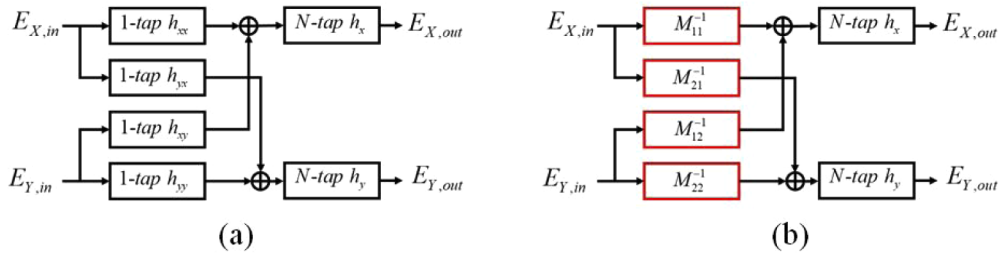


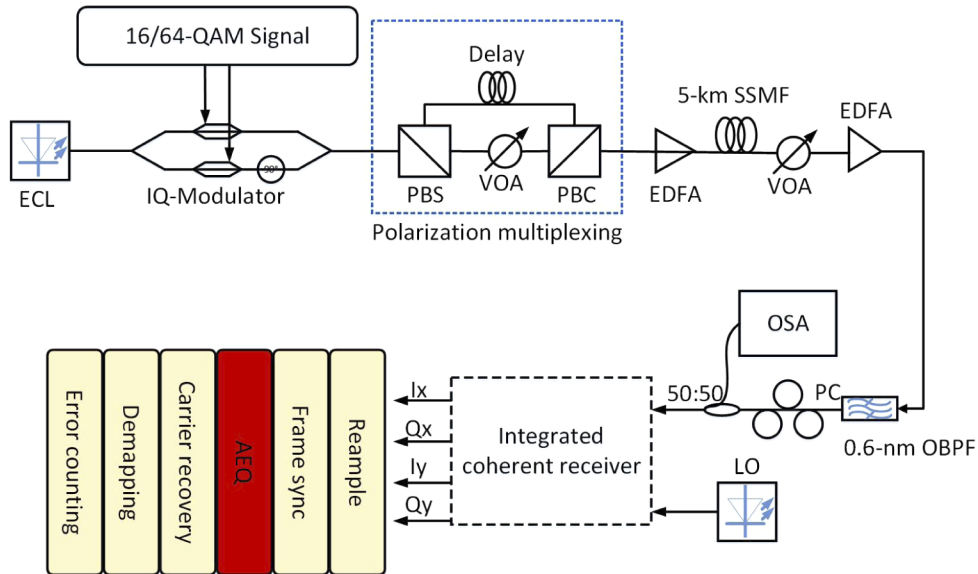
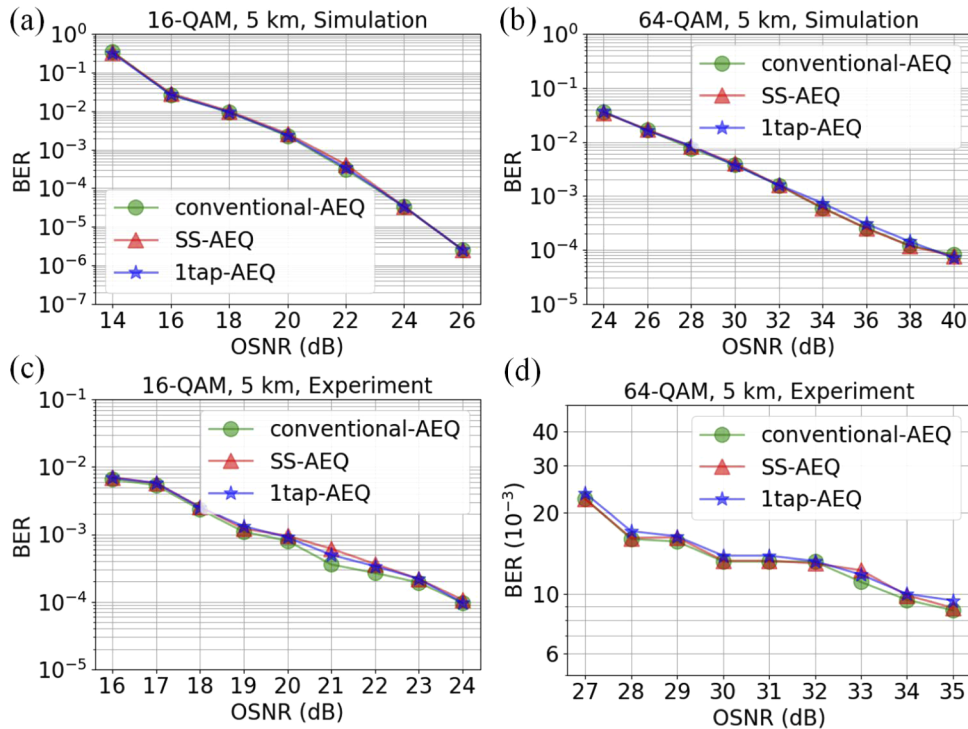
**Fig. 1.** AEQ structure. (a) 1tap-AEQ; (b) SS-AEQ

### 3. Experimental verification

In this section, we verify the performance of proposed SS-AEQ in experiment. On the transmitter side, we use square-root raised-cosine pulse shaping with 0.2 roll-off factor. As shown in Fig. 2, we generate the 12.5 GBaud DP-16/64-QAM optical signal by modulating a carrier signal, provided by an external cavity laser (ECL), using I/Q modulators which are driven by multi-level electrical signals. The center wavelength of ECL is 1552.52 nm and its line-width is 100 kHz. Polarization multiplexing is then realized by utilizing polarization beam splitters (PBSs), polarization beam combiners (PBCs) and optical delay lines. A variable optical attenuator (VOA) is utilized to introduce PDL [17]. The resulting signals are amplified using an erbium-doped fiber amplifier (EDFA) and sent over a 5 km long standard single-mode fiber (SSMF). Another VOA is utilized to alter optical signal-to-noise ratios (OSNRs) in the range of 15~30 dB. The optical signals at the output of EDFA are filtered using a 0.6 nm optical band-pass filter (OBPF) and then detected by a coherent receiver. The electrical signals after optical-to-electronic (O/E) conversion are sampled by utilizing an oscilloscope with 50 Gsamples/s sampling rate.  $2 \times 10^6$  samples are collected and then processed offline. As for offline DSP, after being resampled to 2 samples per symbol and synchronized with transmitted symbols, the signals are fed into AEQ block. Note that we do not utilize fixed CD compensation and CD is compensated by AEQ, which is an important simplification following [7,9] for short reach applications. Next, the carrier phase recovery based on blind phase search (BPS) [18] is performed to remove frequency offset and phase noise. Finally, after symbol mapping and decision, the bit error ratio (BER) is obtained by error counting.

To verify the performance of SS-AEQ, we select conventional-AEQ and 1tap-AEQ for comparison and the results are shown in Fig. 3. Figures 3(a), 3(b) show the BER performance of three AEQs. Note that in simulation, the transmission rate is set at 28 GBaud. For both 16-QAM and 64-QAM signals, three AEQs have very similar performance in both simulation and experiment. Additionally, we analyze the convergence speed of SS-AEQ and 1tap-AEQ and results are shown in Fig. 4. For 1tap-AEQ, the step sizes are  $10^{-3}$  and  $3 \times 10^{-4}$  for PolDemux and mitigating ISI respectively. For SS-AEQ, the step size is also set at  $3 \times 10^{-4}$  for mitigating ISI. Although the two AEQs have similar convergence speed in the stage of mitigating ISI, SS-AEQ outperforms 1tap-AEQ during the stage of PolDemux. As shown in Fig. 4(a), while 1tap-AEQ requires thousands of symbols to become stable, SS-AEQ just requires hundreds of symbols to achieve stable performance, which indicates that SS-AEQ is more adaptable to channel changes.

Finally, we conclude the computational complexity of three AEQs in Table 1, in which the complexity is denoted by the number of real multipliers and  $N$  is the tap number of FIR filters. In our experiment, we set the tap number at 21. Thus the number of real multipliers is 336, 184 and 184 for conventional-AEQ, 1tap-AEQ and SS-AEQ, respectively. In other words, proposed SS-AEQ has the same computational complexity with 1tap-AEQ and reduces the computational complexity of conventional-AEQ by 45.24%. In conclusion, for the systems

**Fig. 2.** Experiment setup and DSP flow.**Fig. 3.** (a) BER vs. OSNR in 16-QAM system with SS-AEQ, conventional-AEQ and 1tap-AEQ; (b) BER vs. OSNR in 64-QAM system with SS-AEQ, conventional-AEQ and 1tap-AEQ.

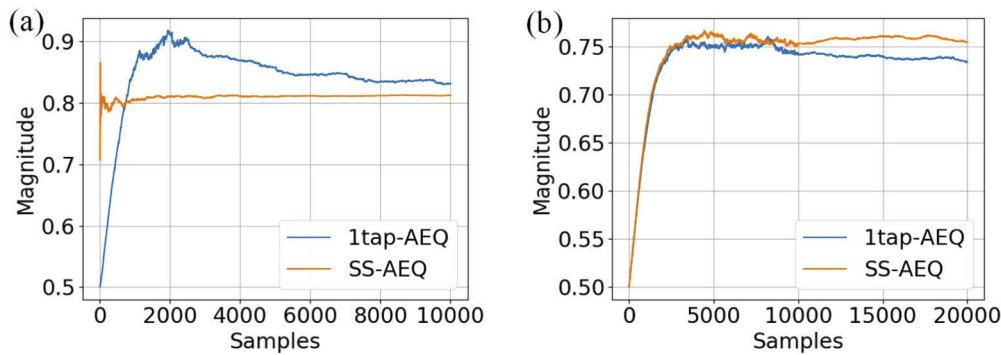


**Fig. 4.** (a) Convergence speed during the stage of PolDemux; (b) convergence speed during the stage of mitigating ISI.

with very short transmission distance such as intra-datacenter applications, SS-AEQ, 1tap-AEQ and conventional-AEQ have very similar performance. Compared with conventional-AEQ, both SS-AEQ and 1tap-AEQ benefit from their two-stage configuration and thus have lower computational complexity. Moreover, SS-AEQ has faster convergence speed than 1tap-AEQ. Next we will analyze the tolerance of PDL and CD for these AEQs to see how they could be extended to other short reach systems.

**Table 1. Number of real multiplications per symbol**

Method	Number of real multipliers
Conventional-AEQ	$16 \times N$
1tap-AEQ	$8 \times N + 16$
SS-AEQ	$8 \times N + 16$

#### 4. Tolerance of PDL and CD

In this section, we numerically analyze the tolerance of PDL and CD for three AEQs.

##### 4.1. Polarization dependent loss

In simulated system, PDL is implemented by a lumped module before the transmission fiber. Its input/output field relation is expressed as:

$$\begin{pmatrix} E_{out,x} \\ E_{out,y} \end{pmatrix} = \mathbf{M} \bullet \begin{pmatrix} \sqrt{1-\rho} & 0 \\ 0 & \sqrt{1+\rho} \end{pmatrix} \bullet \mathbf{M}' \bullet \begin{pmatrix} E_{in,x} \\ E_{in,y} \end{pmatrix}, \quad (5)$$

where  $\mathbf{M}$  and  $\mathbf{M}'$  are two different unitary matrixes to simulate the fiber effect,  $\rho$  is the normalized PDL coefficient and is calculated by  $\rho = (10^{PDL/10} - 1)/(10^{PDL/10} + 1)$ . To simulate the changing state of polarization (SOP) in propagation, we rewrite the unitary matrix  $\mathbf{M}$  in Eq. (1) as

$$\mathbf{M} = \begin{pmatrix} \sqrt{\alpha} \exp(j\delta) & -\sqrt{1-\alpha} \\ \sqrt{1-\alpha} & \sqrt{\alpha} \exp(-j\delta) \end{pmatrix}. \quad (6)$$

Then we sweep  $\alpha$  and  $\delta$  in the range where  $0 \leq \alpha \leq 1$  and  $-\pi \leq \delta \leq \pi$ . In both simulation and experiment, the value of  $\alpha$  and  $\delta$  is adjusted through numerical simulation in offline DSP, i.e. we

apply  $\mathbf{M} \bullet (E_x; E_y)$  as a preprocessing before AEQ, where  $E_x, E_y$  are the received signals at X and Y polarization tributary. The results of PolDemux are shown by colored maps on an  $\alpha - \delta$  plane consisting of  $10 \times 20$  segments. Dark areas represent the cases that PolDemux fail, and the light areas represent the cases that PolDemux is well done. As shown in Figs. 5(a)–5(c), 1tap-AEQ suffers higher risk of wrong PolDemux as the PDL increases. In contrast, from Figs. 5(d)–5(f) we can see that SS-AEQ can always perform robust PolDemux as PDL increases. Also, we use the data from experiment with 1 dB PDL and compare the results between conventional-AEQ [Fig. 5(g)], 1tap-AEQ (h) and SS-AEQ (i). From Fig. 5(g)–5(i), we can see that both 1tap-AEQ and conventional-AEQ suffer from failure of PolDemux, while SS-AEQ performs stable PolDemux. Note that in experiment, we introduce PDL to the system by adjusting a VOA and monitor the value of PDL in offline DSP. In addition, since we transmit the optical signals through a SSMF, the simulated changing SOP represented by  $\mathbf{M}$  [in Eq. (6)] does not start from  $[1, 0; 0, 1]$  and thus the colored maps in this section are not symmetrical.

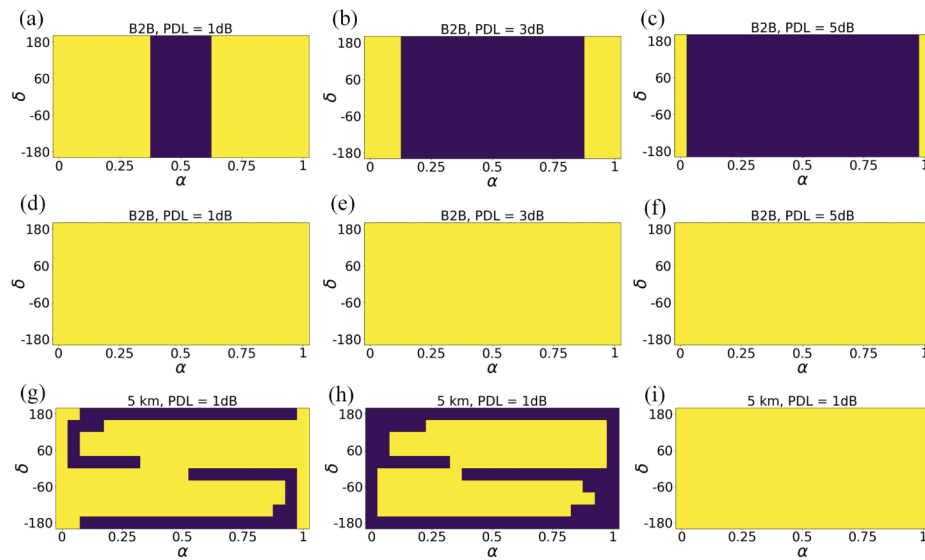


**Fig. 5.** Maps of PolDemux stability with the existence of PDL. (a) Simulated B2B 16-QAM system with 1 dB PDL using 1tap-AEQ; (b) simulated B2B 16-QAM system with 3 dB PDL using 1tap-AEQ; (c) simulated B2B 16-QAM system with 5 dB PDL using 1tap-AEQ; (d) simulated B2B 16-QAM system with 1 dB PDL using SS-AEQ; (e) simulated B2B 16-QAM system with 3 dB PDL using SS-AEQ; (f) simulated B2B 16-QAM system with 5 dB PDL using SS-AEQ; (g) experimental 5 km 16-QAM system with 1 dB PDL using conventional-AEQ; (h) experimental 5 km 16-QAM system with 1 dB PDL using 1tap-AEQ; (i) experimental 5 km 16-QAM system with 1 dB PDL using SS-AEQ.

The failure of PolDemux by CMA-based methods corresponds to the singularity problem [17,10], which means that the butterfly-structured FIR may converge to a situation where the two tributary have the same data. To improve the performance of CMA, several ways have been proposed to prevent CMA from singularity problem [17,19–21]. Constrained CMA [17] and Two-Stage CMA [20] relies on the relationship between elements in a unitary matrix to constrain the tap coefficients. MU-CMA [19] tracks the cross-correlation between equalized signals by adding an additional correlation term to the cost function of CMA. Although these modified CMA-based methods are effective, they cannot ensure total singularity avoidance [21]. Besides non-data-aided methods, there are also data-aided algorithm such as least mean square (LMS) algorithm [22], which can also avoid singularity problem by introducing training symbols to force

a correct recovery. However, the data-aided algorithm has two obvious drawbacks in short-reach systems. First, data-aided approach requires training symbols that contain no information, thus it reduces spectral efficiency. Second, training symbols require strict frame synchronization which increase the DSP complexity and power consumption. In contrast, Stokes-space-based PolDemux ensures singularity avoidance because PDL will not affect the overall shape of signals' distribution in Stokes space [14], and requires no additional training symbols.

To further explore the effect of PDL, we also investigate the relationship between PDL and BER performance for three AEQs. We use data from a 28 GBaud DP-16-QAM system with 5 km transmission in simulation, and adjust  $\alpha$  and  $\delta$  in offline DSP to guarantee successful PolDemux for 1tap-AEQ and conventional-AEQ. As shown in Fig. 6, under the condition of successful PolDemux, both 1tap-AEQ and SS-AEQ suffers from performance loss, while conventional-AEQ has higher tolerance of PDL. From Eq. (5) we can see that PDL introduces additional linear distortion in addition to the polarization rotation, therefore, SS-AEQ has performance degradation when PDL is large. In the next subsection, we explain that the design of loss function for CMA/MMA in the PolDemux stage of 1tap-AEQ is ineffective. While PDL introduces additional distortion, the problem becomes more significant and leads to the performance degradation of 1tap-AEQ.

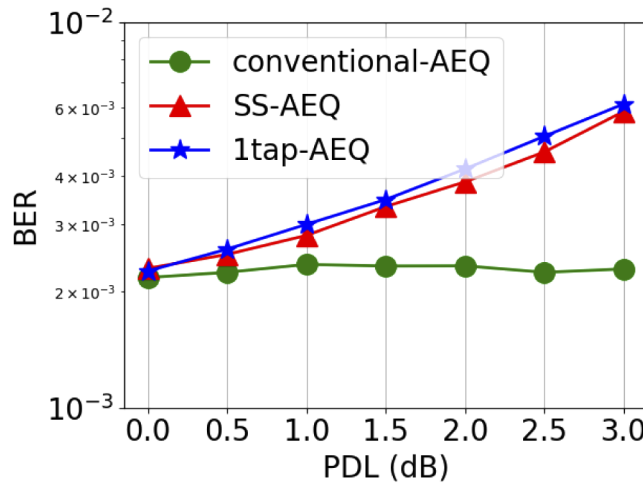


**Fig. 6.** BER vs. PDL in simulated 16-QAM system.

#### 4.2. Chromatic dispersion

The fiber chromatic dispersion is also an important factor that will affect the algorithm performance, especially when fiber length is long. In simulated system, we set the dispersion parameter at  $16 \times 10^{-6} \text{ s/m}^2$ . We compare the BER performance of three different AEQs with transmission from 5 km to 20 km. From Figs. 7(a), 7(b), we can see that SS-AEQ remains stable and similar performance compared with conventional-AEQ. However, the performance of 1tap-AEQ is reduced when transmission distance is large. As shown in Figs. 7(c), 7(d), we can see that in a system with 5 km transmission, the performance of 1tap-AEQ is stable while the step size is changed during PolDemux stage. However, when the transmission distance comes to 20 km, it is extremely difficult to find a proper step size for 1tap-AEQ in the first stage. In other words, 1tap-AEQ is difficult to perform correct PolDemux when CD is large. This problem of 1tap-AEQ can be explained by the following analysis.

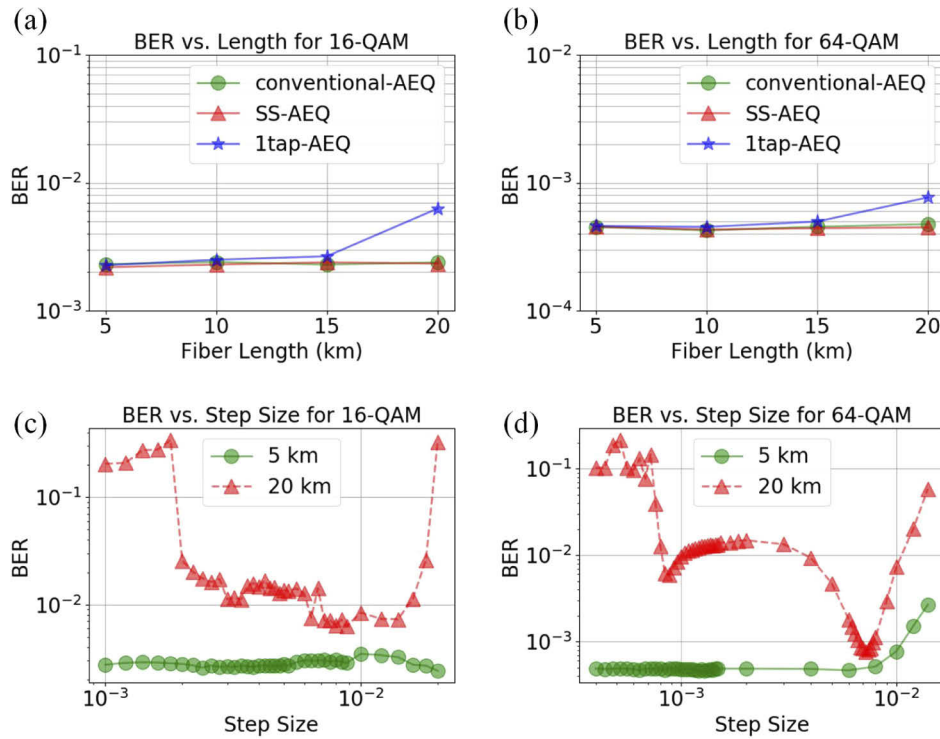


**Fig. 7.** (a) BER vs. fiber length in simulation for SS-AEQ, conventional-AEQ and 1tap-AEQ; (b) BER vs. step size in simulation for 1tap-AEQ; (c) convergence of SS-AEQ and 1tap-AEQ in PolDemux with different transmission distances.

Essentially, the aim of CMA/MMA algorithm is to recover the constellation diagram of QAM signals to multiple rings. In the DSP flow of optical receiver, the constellations of signals are rings like object after successful AEQ [shown in Fig. 8(b)]. Accordingly, the goal of CMA/MMA is to minimize the distance between signals' moduli and their reference moduli. Therefore, the loss function of CMA/MMA is designed as the mean square error (MSE) form and can be written as [23]:

$$L = \frac{1}{N} \sum_{i=1}^N \left[ (|E_i|^2 - R_i^2)^2 \right], \quad (7)$$

where  $L$  denotes the loss function,  $E_i$  is the value of  $i$ th sample of signal,  $R_i$  is the reference modulus for  $i$ th signal and  $N$  is the number of samples. In conventional-AEQ, there is only one stage of transformation for incoming signals. After conventional-AEQ, the constellation diagrams of signals are recovered as Fig. 8(b), and thus the value of  $L$  is obviously low after AEQ. Therefore, it is suitable to use CMA/MMA to perform equalization. In contrast, the 1tap-AEQ has two stages of transformation and both use CMA/MMA, i.e. use  $L$  as loss function to update the tap coefficients. The first stage performs PolDemux and the second stage mitigates ISI. However, in a short reach system where CD is compensated after PolDemux, the goal of CMA/MMA in the first stage is to find the correct inversed polarization rotation matrix, rather than recover the constellation to rings like object. As shown in Fig. 8(a), the signals' constellation after PolDemux is not like rings. Because the design of objective function should reflect the true objective [24], the design of  $L$  is not useful in the first stage of 1tap-AEQ. To verify our inference, we compute the value of  $L$  for signals after correct PolDemux by SS-AEQ, and  $L$  for signals

after correct equalization by conventional-AEQ. As shown in Fig. 9, it is obvious that the value of  $L$  after full AEQ remains low as the fiber length increase. However,  $L$  after only PolDemux increases as the fiber length increase, which explains the performance degradation of 1tap-AEQ when transmission distance is long.

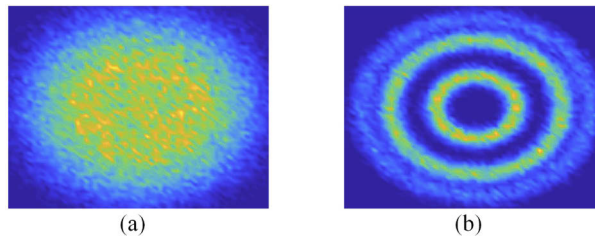


**Fig. 8.** (a) Constellations after PolDemux; (b) constellations after mitigating ISI.

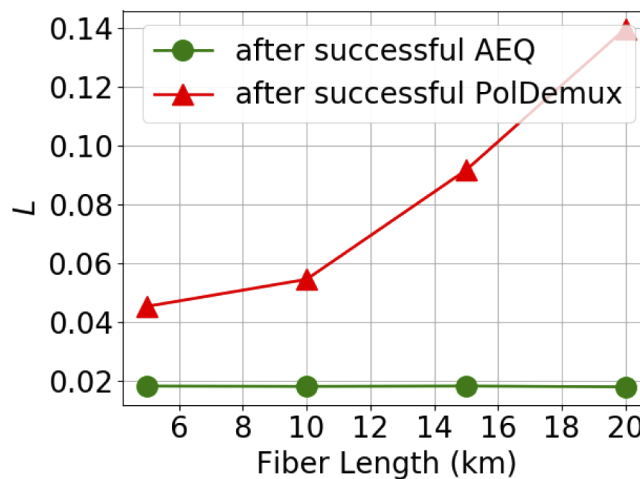


**Fig. 9.**  $L$  in Eq. (7) after AEQ/PolDemux vs. fiber length.

## 5. Conclusion

In this paper, we propose and experimentally demonstrate a PDL and CD insensitive and low-complexity SS-AEQ. It combines Stokes space-based PolDemux with CMA-based channel equalization. According to the experimental results, SS-AEQ has similar BER performance compared with 1tap-AEQ and conventional-AEQ. For computational complexity, SS-AEQ reduces the number of multipliers by  $\sim 45\%$  compared with conventional-AEQ. Although SS-AEQ has similar complexity with 1tap-AEQ, it will not suffer from failure of PolDemux and has faster convergence speed. In addition, according to our numerical analysis, SS-AEQ is insensitive to CD with transmission of at least 20 km SSMF, while 1tap-AEQ suffers from performance loss when fiber length is longer than 15 km. Therefore, proposed AEQ is attractive and robust for next generation short reach applications.

**Funding.** National Key Research and Development Program of China (2019YFB1803504); National Natural Science Foundation of China (61821001, 61901045, 61625104, 61801037); Fundamental Research Funds for the Central Universities (2019RC11).

**Disclosures.** The authors declare no conflicts of interest.

## References

1. K. Kikuchi, "Fundamentals of Coherent Optical Fiber Communications," *J. Lightwave Technol.* **34**(1), 157–179 (2016).
2. E. El-Fiky, M. Chagnon, M. Sowailem, A. Samani, M. Morsy-Osman, and D. V. Plant, "168-Gb/s Single Carrier PAM4 Transmission for Intra-Data Center Optical Interconnects," *IEEE Photonics Technol. Lett.* **29**(3), 314–317 (2017).
3. R. Lin, J. Van Kerrebrouck, X. Pang, M. Verplaetse, O. Ozolins, A. Udalcovs, L. Zhang, L. Gan, M. Tang, S. Fu, R. Schatz, U. Westergren, S. Popov, D. Liu, W. Tong, T. De Keulenaer, G. Torfs, J. Bauwelinck, X. Yin, and J. Chen, "Real-time 100 Gbps//core NRZ and EDB IM/DD transmission over multicore fiber for intra-datacenter communication networks," *Opt. Express* **26**(8), 10519–10526 (2018).
4. J.-P. Elbers, N. Eiselt, N. Eiselt, A. Dochhan, D. Rafique, and H. Grießer, "PAM4 vs Coherent for DCI Applications," in *Advanced Photonics 2017 (IPR, NOMA, Sensors, Networks, SPPCom, PS)* (2017), Paper SpTh2D.1 (Optical Society of America, 2017), p. SpTh2D.1.
5. M. Morsy-Osman and D. V. Plant, "A Comparative Study of Technology Options for Next Generation Intra- and Inter-datacenter Interconnects," in *Optical Fiber Communication Conference* (OSA, 2018), p. W4E.1.
6. J. Cheng, C. Xie, Y. Chen, X. Chen, M. Tang, and S. Fu, "Comparison of Coherent and IMDD Transceivers for Intra Datacenter Optical Interconnects," in *Optical Fiber Communication Conference (OFC) 2019* (OSA, 2019), p. W1F.2.
7. K. Matsuda, R. Matsumoto, and N. Suzuki, "Hardware-Efficient Adaptive Equalization and Carrier Phase Recovery for 100-Gb/s//λ-Based Coherent WDM-PON Systems," *J. Lightwave Technol.* **36**(8), 1492–1497 (2018).
8. J. Cheng, C. Xie, M. Tang, and S. Fu, "A Low-Complexity Adaptive Equalizer for Digital Coherent Short-Reach Optical Transmission Systems," in *Optical Fiber Communication Conference (OFC) 2019* (OSA, 2019), p. M3H.2.
9. J. Cheng, C. Xie, M. Tang, and S. Fu, "Hardware Efficient Adaptive Equalizer for Coherent Short-Reach Optical Interconnects," *IEEE Photonics Technol. Lett.* **31**(15), 1249–1252 (2019).
10. K. Kikuchi, "Performance analyses of polarization demultiplexing based on constant-modulus algorithm in digital coherent optical receivers," *Opt. Express* **19**(10), 9868–9880 (2011).
11. P. Serena, S. Musetti, S. Almonacil, S. Bigo, A. Benoni, P. Jenneve, N. Rossi, and P. Ramantanis, "The Gaussian Noise Model Extended to Polarization Dependent Loss and its Application to Outage Probability Estimation," in *2018 European Conference on Optical Communication (ECOC)* (IEEE, 2018), pp. 1–3.
12. Z. Tao, L. Dou, T. Hoshida, and J. C. Rasmussen, "A Fast Method to Simulate the PDL Impact on Dual-Polarization Coherent Systems," *IEEE Photonics Technol. Lett.* **21**(24), 1882–1884 (2009).
13. C. Xie, "Polarization-Dependent Loss Induced Penalties in PDM-QPSK Coherent Optical Communication Systems," in *Optical Fiber Communication Conference* (OSA, 2010), p. OWE6.
14. B. Szafraniec, B. Nebendahl, and T. Marshall, "Polarization demultiplexing in Stokes space," *Opt. Express* **18**(17), 17928–17939 (2010).
15. N. J. Muga and A. N. Pinto, "Digital PDL Compensation in 3D Stokes Space," *J. Lightwave Technol.* **31**(13), 2122–2130 (2013).
16. Z. Yu, X. Yi, Q. Yang, M. Luo, J. Zhang, L. Chen, and K. Qiu, "Polarization demultiplexing in stokes space for coherent optical PDM-OFDM," *Opt. Express* **21**(3), 3885–3890 (2013).
17. L. Liu, Z. Tao, W. Yan, S. Oda, T. Hoshida, and J. C. Rasmussen, "Initial Tap Setup of Constant Modulus Algorithm for Polarization De-multiplexing in Optical Coherent Receivers," in *Optical Fiber Communication Conference and National Fiber Optic Engineers Conference* (OSA, 2009), p. OMT2.
18. T. Pfau, S. Hoffmann, and R. Noe, "Hardware-Efficient Coherent Digital Receiver Concept With Feedforward Carrier Recovery for M-QAM Constellations," *J. Lightwave Technol.* **27**(8), 989–999 (2009).
19. A. Vgenis, C. S. Petrou, C. B. Papadias, I. Roudas, and L. Raptis, "Nonsingular Constant Modulus Equalizer for PDM-QPSK Coherent Optical Receivers," *IEEE Photonics Technol. Lett.* **22**(1), 45–47 (2010).
20. C. Xie and S. Chandrasekhar, "Two-Stage Constant Modulus Algorithm Equalizer for Singularity Free Operation and Optical Performance Monitoring in Optical Coherent Receiver," in *Optical Fiber Communication Conference* (OSA, 2010), p. OMK3.
21. V. N. Rozental, T. F. Portela, D. V. Souto, H. B. Ferreira, and D. A. A. Mello, "Experimental analysis of singularity-avoidance techniques for CMA equalization in DP-QPSK 112-Gb/s optical systems," *Opt. Express* **19**(19), 18655–18664 (2011).
22. S. J. Savory, "Digital Coherent Optical Receivers: Algorithms and Subsystems," *IEEE J. Sel. Top. Quantum Electron.* **16**(5), 1164–1179 (2010).
23. J. Yang, J.-J. Werner, and G. A. Dumont, "The multimodulus blind equalization and its generalized algorithms," *IEEE J. Sel. Area. Comm.* **20**(5), 997–1015 (2002).
24. G. Hinton, O. Vinyals, and J. Dean, "Distilling the Knowledge in a Neural Network," arXiv:1503.02531 [cs, stat] (2015).